



# Rare-earth metal compounds with a novel ligand 2-methoxycinnamylidenepyruvate: A thermal and spectroscopic approach



C.T. Carvalho<sup>a,\*</sup>, G.F. Oliveira<sup>a</sup>, J. Fernandes<sup>a,b,c,d</sup>, A.B. Siqueira<sup>b</sup>, E.Y. Ionashiro<sup>c</sup>, M. Ionashiro<sup>d</sup>

<sup>a</sup> Federal University of Grande Dourados, UFGD, 79.804-970 Dourados, MS, Brazil

<sup>b</sup> Federal University of Mato Grosso, UFMT, 78.060-900 Cuiabá, MT, Brazil

<sup>c</sup> Federal University of Goiás, UFG, 74.690-900, Goiânia, GO, Brazil

<sup>d</sup> Institute of Chemistry, UNESP, 14.801-970 Araraquara, SP, Brazil

## ARTICLE INFO

### Article history:

Received 26 January 2016

Received in revised form 10 May 2016

Accepted 13 May 2016

Available online 14 May 2016

### Keywords:

Lanthanide

2-Methoxycinnamylidenepyruvate

Compounds

TG-DTA/FT-IR

TG-DTA/MS

## ABSTRACT

Compounds of 2-methoxycinnamylidenepyruvate with trivalent lanthanide ions (Tb, Ho, Er, Tm, Yb and Lu) were obtained in solid state and studied mainly in terms of their thermal and spectroscopic properties. The analyses of the characterization were performed by thermogravimetric system coupled to a mass and infrared spectrometer (TG-DTA/MS and TG-DTA/FT-IR), X-ray powder diffractometry, differential scanning calorimetry (DSC), infrared (FT-IR), preliminary study of fluorescence as well as classical technique of titration with EDTA. From these results, it was possible to establish the stoichiometry, thermal behavior, hydration water content, and the gaseous products released in the thermal decomposition steps, and suggest the type of metal-ligand coordination.

© 2016 Elsevier B.V. All rights reserved.

## 1. Introduction

Rare earths like the lanthanide ions are known to have great importance for high technology industry due to their employment in several electronic devices with civil and military applications. These ions form chemically stable compounds with organic ligands besides presenting excellent thermal stability and well-defined structural arrangements when complexed with carboxylate ligands [1–9].

In this study, the organic ligand 2-methoxycinnamylidenepyruvate (2-MeO-HCP), obtained from aldolic condensation of cinnamic acid and pyruvate, was used to synthesize the compounds in solid state with heavy trivalent lanthanides. The synthesis and characterization of 2-MeO-HCP and other compounds have been reported in previous studies [10–12] which aimed at fundamentally performing the synthesis and investigation of the compounds in solid state by the establishment of stoichiometry, thermal behavior and thermal

decomposition, FT-IR spectroscopy and the classical analysis method of titration with EDTA. In this paper, the compounds of lanthanides 2-methoxycinnamylidenepyruvate were studied using the techniques mentioned, as well as employing complementary techniques like X-ray powder diffraction to provide qualitative information on the crystallinity of the compounds and mass spectrometry coupled to a thermogravimetric system (TG/MS) to support the gases analysis performed by TG/FT-IR on the gases evolved from the samples undergone thermal decomposition process. Preliminary fluorescence study of the compounds and its salt was performed with the optimum wavelength of emission and excitation. Regarding the groups coordinated to the metal, it was possible to confirm which atoms are responsible for the energy transfer to the lanthanide ions. These compounds have attracted attention due to the magnetic and spectroscopic properties of lanthanide ions and their complexes, which make them have a wide range of applications, as reported in the literature, and also promising for future biological uses [13,14].

\* Corresponding author.

E-mail address: [claudiocarvalho@ufgd.edu.br](mailto:claudiocarvalho@ufgd.edu.br) (C.T. Carvalho).

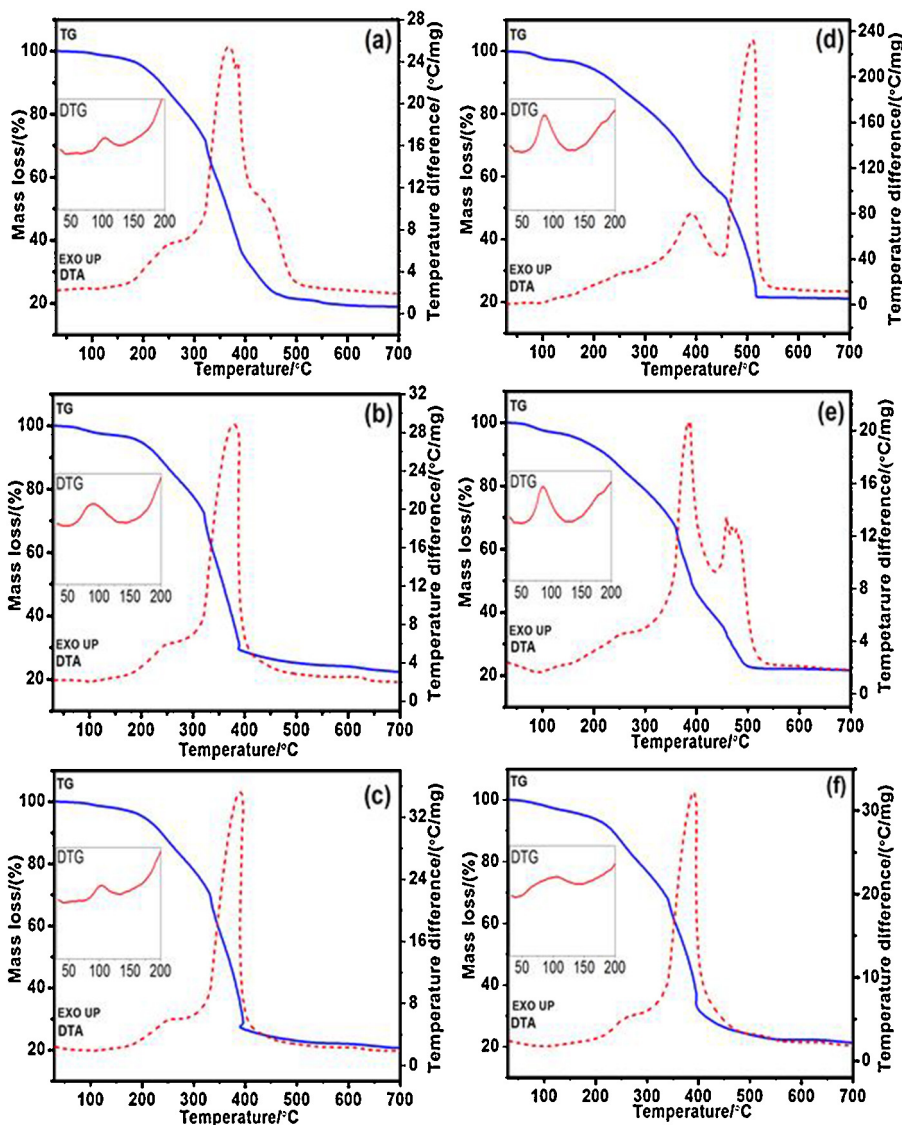


**Fig. 1.** TG–DTA curves and DTG curves between 30 and 200 °C to signalize the event with hydration water loss for each compound: (a)  $\text{Tb}(\text{L})_3 \cdot \text{H}_2\text{O}$  ( $m = 7.84 \text{ mg}$ ), (b)  $\text{Ho}(\text{L})_3 \cdot \text{H}_2\text{O}$  ( $m = 7.28 \text{ mg}$ ), (c)  $\text{Er}(\text{L})_3 \cdot \text{H}_2\text{O}$  ( $m = 7.65 \text{ mg}$ ), (d)  $\text{Tm}(\text{L})_3 \cdot 1.5\text{H}_2\text{O}$  ( $m = 7.27 \text{ mg}$ ), (e)  $\text{Yb}(\text{L})_3 \cdot 1.5\text{H}_2\text{O}$  ( $m = 7.20 \text{ mg}$ ), (f)  $\text{Lu}(\text{L})_3 \cdot 1.5\text{H}_2\text{O}$  ( $m = 7.66 \text{ mg}$ )  $\text{L} = 2$ -methoxycinnamylidenepyruvate.

## 2. Experimental

### 2.1. Synthesis of the organic ligand

The 2-methoxycinnamaldehyde,  $(\text{CH}_3\text{O}-\text{C}_6\text{H}_4-(\text{CH})_2-\text{CHO})$  96% pure predominantly trans, was obtained from Aldrich and sodium pyruvate ( $\text{H}_3\text{C}-\text{CO}-\text{COONa}$ ) 99% pure from Sigma.

Sodium 2-methoxycinnamylidenepyruvate ( $\text{Na}-2-\text{MeO}-\text{CP}$ ) and its corresponding acid were both synthesized following the procedure described in the literature [10], with some modifications which include an aqueous solution of sodium pyruvate (8.71 g per 10 mL) added under continuous stirring to 20 mL of methanolic solution of 2-methoxycinnamaldehyde (13.23 g). Sixty-three milliliters of an aqueous sodium hydroxide solution 5% (m/v) was slowly added while the reacting system was stirred and cooled in an ice bath. The addition rate of alkali was regulated so that the temperature remained between 5 and 9 °C. The formation of a pale yellow precipitate was observed during the addition of sodium hydroxide solution.

The system was left to stand for about 3 h at temperature between 23 and 25 °C. The pale yellow precipitate (impure sodium 2-methoxycinnamylidenepyruvate) was filtered and washed with 100 mL portions of methanol to remove most of the unreacted aldehyde and secondary products. The crude product was dissolved in water (200 mL) and concentrated hydrochloric acid ( $12 \text{ mol L}^{-1}$ ) was added to the solutions under continuous stirring until total precipitation of 2-methoxycinnamylidenepyruvic acid (4.8 g).

Aqueous solution of  $\text{Na}-2-\text{MeO}-\text{CP}$   $0.1 \text{ mol L}^{-1}$  was prepared by direct weighing of the salt. Lanthanide chlorides were prepared from the corresponding metal oxides by treatment with concentrated hydrochloric acid. The resulting solutions were evaporated to near dryness to eliminate the excess of hydrochloric acid. The residues were redissolved in distilled water, transferred to a volumetric flask and then diluted in order to obtain ca.  $0.100 \text{ mol L}^{-1}$  solutions, whose pH was adjusted to around 5 by adding diluted sodium hydroxide or hydrochloric acid solutions. The yield of the ligand was estimated at approximately 28%.

## 2.2. Synthesis of the compounds

The solid-state compounds were prepared by slowly adding the solution of ligand to the respective metal chloride under continuous stirring until total precipitation of the metal ions. The precipitates were washed out with distilled water until total elimination of chloride ions. These were then filtered through and dried on Whatman n° 42 filter paper and kept in a desiccator over anhydrous calcium chloride. The yield of the compound when synthesized using stoichiometric proportions of ligand and metal was about 80–90%. This percentage is due to losses occurred during washing.

## 2.3. Characterization of the compounds

The content of metal ions were also determined by complexometric titration with standard EDTA solution and xylenol orange as indicator [15,16] after igniting the compounds to their respective oxides and then dissolving them in hydrochloric acid solution. For complexometric titration, the pH of the solution containing the metal ions was adjusted between 5 and 6. The carbon and hydrogen contents were determined by elemental analysis using a Fison EA 1108 CNHS–O instrument.

X-ray powder patterns were obtained using a Siemens D-5000 X-ray diffractometer, employing CuK $\alpha$  radiation ( $\lambda = 1.541 \text{ \AA}$ ) and a setting of 40 kV and 20 mA.

Infrared spectra for Na-2-MeO-CP, as well as for its metal-ion compounds were run on a Nicolet Model Impact 400 FTIR instrument within the 4000–400  $\text{cm}^{-1}$  range. The solid samples were pressed into KBr pellets.

Simultaneous TG–DTA and DSC curves were obtained by two thermal analysis systems, models SDT 2960 and DSC Q10, both from TA Instruments. The purge gas was an air flow of 100  $\text{mL min}^{-1}$  for TG–DTA and 50  $\text{mL min}^{-1}$  for DSC. A heating rate of 20  $^{\circ}\text{C min}^{-1}$  for TG–DTA and 40  $^{\circ}\text{C min}^{-1}$  for DSC was adopted, with samples weighing about 7 mg for TG–DTA and 5 mg for DSC. Alumina and aluminium crucibles, the latter with perforated covers, were used for TG–DTA and DSC respectively.

Coupled TG–MS measurements were carried out using TA Instruments SDT 2960 simultaneous TG–DTA unit with a heating rate of 5  $^{\circ}\text{C min}^{-1}$  and helium purging (10  $\text{L h}^{-1}$ ) and a Balzers thermostat GSD 300T quadrupole mass spectrometer with a heated silica capillary inlet, which was used in multiple ion detection (MID) mode when fragments with previously adjusted m/e values were followed.

For the fluorescence studies, a Varian Cary Eclipse spectrofluorimeter was used applying an excitation scan in the range of 210 nm to 600 nm at intervals of 10 nm. A xenon lamp with two monochromators was used as excitation source, one of which was intended for selecting the excitation wavelength and the other for selecting the wavelength emitted by the sample, with fluorescence detection by a photomultiplier tube.

It were solubilized 5 mg of each compound in dimethylformamide 99% purity (J.T. Baker) and analyzed at a temperature of 25  $^{\circ}\text{C}$ .

Absorption spectra in the visible region were recorded using a bench spectrophotometer (Varian Cary 50<sup>®</sup>) equipped with a xenon lamp as excitation source and a quartz cell with 10 mm path length at 25  $^{\circ}\text{C}$ .

## 3. Results and discussion

### 3.1. Thermal analysis

Simultaneous TG–DTA curves of the compounds are shown in Fig. 1(a–f). Additionally, insets in Fig. 1 show close-up views of the

**Table 1**

Temperature ranges ( $\theta$ ), mass losses ( $\Delta m$ ) and peak temperatures observed for each step of the TG–DTA curves of the compounds  $\text{Ln}(\text{L})_3 \cdot n\text{H}_2\text{O}$ , where Ln = heavy lanthanides and n = number of water molecules.

Compounds		Steps $^{\circ}\text{C}$				
		First	Second	Third	Fourth	Fifth
$\text{Tb}(\text{L})_3 \cdot \text{H}_2\text{O}$	$\theta$ $^{\circ}\text{C}$	30–120	120–300	300–396	396–510	510–700
	$\Delta m$ (%)	1.76	27.82	47.05	2.83	0.77
	Peak ( $^{\circ}\text{C}$ )	110	250	366,383	410–505	–
$\text{Ho}(\text{L})_3 \cdot \text{H}_2\text{O}$	$\theta$ $^{\circ}\text{C}$	30–120	120–300	300–396	396–505	505–700
	$\Delta m$ (%)	2.10	26.18	46.14	4.24	2.31
	Peak ( $^{\circ}\text{C}$ )	100	248	380	–	–
$\text{Er}(\text{L})_3 \cdot \text{H}_2\text{O}$	$\theta$ $^{\circ}\text{C}$	30–120	120–300	300–396	396–607	607–700
	$\Delta m$ (%)	1.80	28.36	42.60	4.28	2.56
	Peak ( $^{\circ}\text{C}$ )	110	250	390	–	–
$\text{Tm}(\text{L})_3 \cdot 1.5\text{H}_2\text{O}$	$\theta$ $^{\circ}\text{C}$	30–120	120–350	350–396	396–520	–
	$\Delta m$ (%)	2.81	22.45	20.85	33.19	–
	Peak ( $^{\circ}\text{C}$ )	86	–	390	510	–
$\text{Yb}(\text{L})_3 \cdot 1.5\text{H}_2\text{O}$	$\theta$ $^{\circ}\text{C}$	30–120	120–350	350–396	396–503	503–700
	$\Delta m$ (%)	2.77	31.00	39.64	5.67	0.6
	Peak ( $^{\circ}\text{C}$ )	95	260	380–387	458–486	–
$\text{Lu}(\text{L})_3 \cdot 1.5\text{H}_2\text{O}$	$\theta$ $^{\circ}\text{C}$	30–120	120–350	350–396	396–555	555–700
	$\Delta m$ (%)	2.81	30.49	33.64	10.93	1.14
	Peak ( $^{\circ}\text{C}$ )	100	265	390	525	–

DTG curves in order to highlight the endothermic event in the first decomposition step.

The first mass losses are due to hydration water, which respective percentages observed in Table 1 can be identified in the TG curves (30–120  $^{\circ}\text{C}$ ) and associated with the broad endothermic events in the DTA curves with a maximum peak near 100  $^{\circ}\text{C}$ . These mass losses occur in a single step and through a slow process similar to compounds obtained in amorphous state, as previously reported in studies involving rare earth ions [17,18].

For the second steps, the thermal decomposition occurs in three (Tm) or four (Tb, Ho, Er, Yb, Lu) overlapping steps. The thermal events are observed between 120 and 300  $^{\circ}\text{C}$  (Tb, Ho, Er) and between 120 and 350  $^{\circ}\text{C}$  (Tm, Yb, Lu) in the TG–DTA curves. These thermal events occur through a slow process, corresponding to small and broad exothermic events ascribed to the decarboxylation of the ligand. For the three steps, the thermal events in TG–DTA curves occur through overlapping and consecutive process and with intense exothermic peaks, except for thulium compound, which showed less intense peak at 390  $^{\circ}\text{C}$ , probably also related to the decarboxylation process. The intense peaks in respective DTA curves observed at 366 and 383  $^{\circ}\text{C}$  (Tb), 380  $^{\circ}\text{C}$  (Ho), 390  $^{\circ}\text{C}$  (Er, Lu), 380 and 387  $^{\circ}\text{C}$  (Yb) are due to the oxidation and/or combustion of the organic matter with production of carbon dioxide and other volatiles of small molar mass detected by the TG/FT-IR and TG/MS systems.

From the fourth steps, some more relevant discrepancies can be observed in TG–DTA curves for the thermal decomposition ranges, which are observed between 396 and 510  $^{\circ}\text{C}$  (Tb), 396 and 505  $^{\circ}\text{C}$  (Ho), 396 and 607  $^{\circ}\text{C}$  (Er), 396 and 520  $^{\circ}\text{C}$  (Tm), 396 and 503  $^{\circ}\text{C}$  (Yb), 396 and 555  $^{\circ}\text{C}$  (Lu). Thulium and ytterbium compounds decompose without formation of residue and with small formation of remaining material (0.6 mg), respectively. Therefore, the last thermal decomposition steps for the compounds, up to 700  $^{\circ}\text{C}$ , are due to formation of stable intermediates compounds, such as mixture of the respective oxides, carbonaceous residue and a carbonate derivative in a simple non-stoichiometric relation leading to formation of the respective oxides. The data regarding the mass losses in each step in TG curves for all compounds along with their respective thermal events in DTA curves are detailed in Table 1.

**Table 2**  
Content of comparative data obtained from instrumental and classic techniques.

Compounds	Ln/(%)			L/(lost) (%)		H <sub>2</sub> O/(%)		C/(%)		H/(%)		Oxides
	Calcd.	TG	EDTA	Calcd.	TG	Calcd	TG	Calcd	EA	Calcd	EA	
Tb(L) <sub>3</sub> ·H <sub>2</sub> O	18.25	17.97	18.46	79.68	78.47	2.07	1.76	53.80	54.41	3.83	3.67	Tb <sub>4</sub> O <sub>7</sub>
Ho(L) <sub>3</sub> ·H <sub>2</sub> O	18.81	19.23	18.95	79.13	78.87	2.05	2.10	53.43	53.17	3.80	3.67	Ho <sub>2</sub> O <sub>3</sub>
Er(L) <sub>3</sub> ·H <sub>2</sub> O	19.03	18.71	19.38	78.92	77.80	2.05	1.80	53.29	53.45	3.79	3.82	Er <sub>2</sub> O <sub>3</sub>
Tm(L) <sub>3</sub> ·1.5H <sub>2</sub> O	18.99	19.00	19.36	77.97	76.49	3.03	2.81	52.65	52.39	3.75	3.86	Tm <sub>2</sub> O <sub>3</sub>
Yb(L) <sub>3</sub> ·1.5H <sub>2</sub> O	19.36	18.72	19.53	77.61	76.91	3.02	2.77	52.40	52.72	3.73	3.78	Yb <sub>2</sub> O <sub>3</sub>
Lu(L) <sub>3</sub> ·1.5H <sub>2</sub> O	19.49	19.34	19.76	77.45	76.20	3.02	2.81	52.32	52.59	3.72	3.85	Lu <sub>2</sub> O <sub>3</sub>

Ln: trivalent lanthanides; L: 2-methoxycinnamylidenepyruvate.

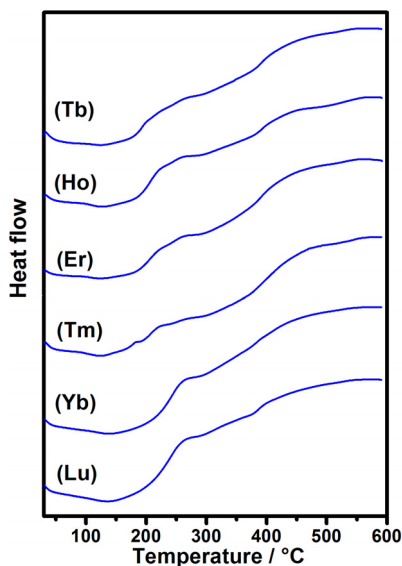


**Fig. 2.** DSC curves of the compounds: Tb(L)<sub>3</sub>·H<sub>2</sub>O (m=5,07 mg), Ho(L)<sub>3</sub>·H<sub>2</sub>O (m=5,23 mg), Er(L)<sub>3</sub>·H<sub>2</sub>O (m=4,95 mg), Tm(L)<sub>3</sub>·1.5H<sub>2</sub>O (m=5,22 mg), Yb(L)<sub>3</sub>·1.5H<sub>2</sub>O (m=4,88 mg), Lu(L)<sub>3</sub>·1.5H<sub>2</sub>O (m=5,30 mg). L=2-methoxycinnamylidenepyruvate.

The thermal data were supported by analyses like complexometric titration with standard EDTA solution and elemental analysis, in order to establish the stoichiometry of the compounds. EDTA titration was used to determine the metal content present in a given mass of a compound, while elemental analysis was used to determine the content of carbon and hydrogen in terms of percentage. The data obtained by these techniques were compared with the thermogravimetric data and displayed in Table 2. These results allowed to establish the stoichiometry of the compounds, which is in agreement with the general formula Ln(2-MeO-CP)<sub>3</sub>·nH<sub>2</sub>O, where Ln represents trivalent lanthanides, 2-MeO-CP is 2-methoxycinnamylidenepyruvate and n is equal to 1 for Tb, Ho, Er and 1.5 for Tm, Yb, Lu.

### 3.2. DSC

The DSC curves of compounds are shown in Fig. 2. A heating rate of 40 °C min<sup>-1</sup> was adopted because no thermal event due to dehydration was observed using a heating rate of 20 °C min<sup>-1</sup>. Despite this, the endothermic peaks attributed to dehydration obtained with a higher heating rate were not sufficient to produce a peak sharper rather than broad. However, it is possible to identify temperature peaks in DSC curves at 120 °C 126 °C (Tb, Ho, Er, Tm), 138 °C (Yb) and 141 °C (Lu). A higher heating rate was chosen due to the fact that events related to dehydration are not dependent on lower heating rates, once a slow heat exchange along the first step in a relatively long time interval is insufficient to produce thermal events. Moreover, DSC curves of the thermal decomposition are different

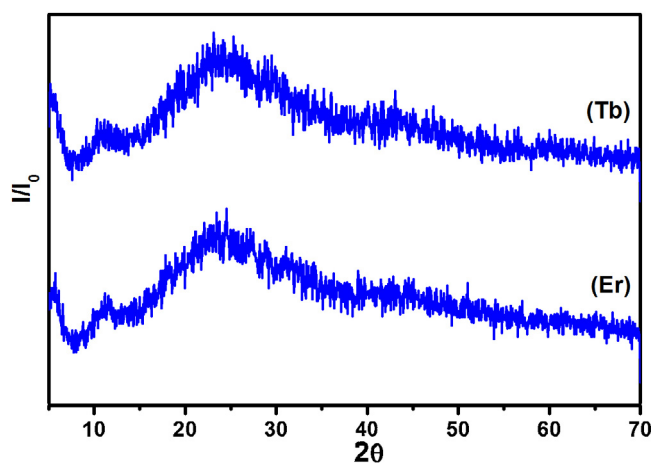


**Fig. 3.** X-ray powder patterns for Tb(L)<sub>3</sub>·H<sub>2</sub>O and Er(L)<sub>3</sub>·H<sub>2</sub>O as representative of all compounds. L=2-methoxycinnamylidenepyruvate.

from the DTA ones. The difference between the curves profiles is indubitably caused by the crucible with perforated cover, as well as by the higher heating rate used to recording DSC curves.

From these data, it was found the following dehydration enthalpies for the compounds, 10.3 (Tb), 17.7 (Ho), 12.9 (Er), 20.4 (Tm), 21.5 (Yb) and 21.5 (Lu) kJ mol<sup>-1</sup> respectively.

### Spectroscopic analyses

#### 3.3. X-ray

The X-ray amorphous powder diffraction patterns, as representative of all compounds are shown in Fig. 3. The X-ray diffractions show a broad halo pattern with the absence of peaks, characteristic of amorphous form. The amorphous state is indubitably related to the low solubility of these compounds, as already observed for lanthanides with other phenyl-substituted derivatives of cinnamylidenepyruvate [19,20].

#### 3.4. FT-IR

In an attempt to suggest the likely coordination mode, analysis by FT-IR spectroscopy of sodium 2-methoxycinnamylidenepyruvate and its compounds were considered in this work, based on the stretching frequencies of the carboxylate and ketonic groups, as well as on the ligand salt.

The infrared spectroscopic data for heavy trivalent lanthanides are shown in Table 3. The investigation focused mainly on the range 1400–1700 cm<sup>-1</sup> because this region provided information on both groups. For sodium 2-methoxycinnamylidenepyruvate, the bands centered at 1668 cm<sup>-1</sup> (ketonic carbonyl stretching) and 1583 cm<sup>-1</sup> (anti-symmetrical carboxylate vibration) are both shifted to lower frequencies in complexes, namely between 1637 and 1654 cm<sup>-1</sup> and 1554–1581 cm<sup>-1</sup> respectively, suggesting lan-

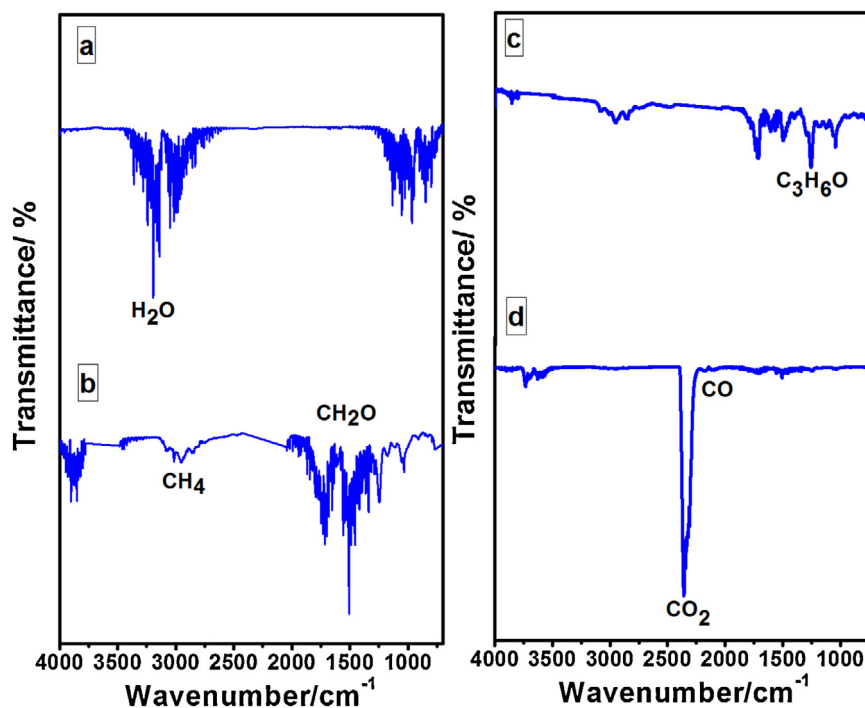


**Fig. 4.** FT-IR two-dimensional (a–d) spectra of the main gaseous products remaining evolved during the thermal decomposition of the terbium and erbium compounds as representative of all samples, between 30 and 700 °C (TG).

**Table 3**

Spectroscopic data for sodium 2-methoxycinnamylidenepyruvate and for its compounds with heavy trivalent lanthanides spectra/cm<sup>-1</sup>.

Compounds	$\nu_{C=O}^a$	$\nu_{asym(COO^-)}^b$	$\nu_{sym(COO^-)}^c$
Na(L) <sub>3</sub> ·H <sub>2</sub> O	1668 <sub>s</sub>	1583 <sub>s</sub>	1402 <sub>s</sub>
Tb(L) <sub>3</sub> ·H <sub>2</sub> O	1654 <sub>s</sub>	1581 <sub>s</sub>	1420 <sub>s</sub>
Ho(L) <sub>3</sub> ·H <sub>2</sub> O	1641 <sub>s</sub>	1556 <sub>s</sub>	1420 <sub>s</sub>
Er(L) <sub>3</sub> ·H <sub>2</sub> O	1641 <sub>s</sub>	1558 <sub>s</sub>	1420 <sub>s</sub>
Tm(L) <sub>3</sub> ·1.5H <sub>2</sub> O	1654 <sub>s</sub>	1556 <sub>s</sub>	1420 <sub>s</sub>
Yb(L) <sub>3</sub> ·1.5H <sub>2</sub> O	1639 <sub>s</sub>	1556 <sub>s</sub>	1420 <sub>s</sub>
Lu(L) <sub>3</sub> ·1.5H <sub>2</sub> O	1637 <sub>s</sub>	1554 <sub>s</sub>	1420 <sub>s</sub>

<sup>s</sup>strong.

<sup>a</sup>  $\nu_{C=O}$ : ketonic carbonyl stretching frequency.

<sup>b</sup>  $\nu_{asym(COO^-)}$  and.

<sup>c</sup>  $\nu_{sym(COO^-)}$ : anti-symmetrical vibrations and symmetrical of the COO<sup>-</sup> group.

thanide coordination both by  $\alpha$ -ketonic carbonyl and carboxylate groups of the ligand [20,21]. This conclusion is supported by the study performed for the lanthanide compounds with the ligand 2-chlorobenzylidenepyruvate. Thus, these data allow to suggest that the lanthanide ions are coordinated to the carboxylate group as bidentate chelating with formation of five membered rings [22].

The gaseous products from thermal decomposition of compounds were monitored by infrared (FT-IR) and mass spectrometry (MS) coupled to TG system techniques. The product identified by FT-IR in the first decomposition step of compounds was only water (TG) followed by carbon monoxide and carbon dioxide along with a small amount of acetone, formaldehyde and methane, evolved during the thermal decomposition process from 200 up to 400 °C. The products like carbon dioxide (CO<sub>2</sub>) and carbon monoxide (CO) shown in two-dimensional (a–d) FT-IR spectra, Fig. 4, were monitored by their characteristic peaks at 2360 and 2400 cm<sup>-1</sup> in the doublet shape and by peak at 666 cm<sup>-1</sup>, while carbon monoxide with one doublet at 2100 and 2180 cm<sup>-1</sup>. Fig. 4 also shows the other gaseous products identified in smaller percentages, like acetone, probably produced from keto group of the ligand presents peaks at 1737 cm<sup>-1</sup>, 1366 cm<sup>-1</sup> and 1215 cm<sup>-1</sup>, which are assigned

to the stretching vibration of C=O, angular symmetric deformation vibration of CH<sub>3</sub> group and angular deformation of C–CO–C group, respectively. For formaldehyde, one intense sharp peak at 1500 cm<sup>-1</sup> between lower intensity sharp peaks of intensity lower at around 1500 cm<sup>-1</sup> can be used to identify the formaldehyde in fingerprint region, whereas for methane these peaks are observed in the region at 3000 cm<sup>-1</sup>, corresponding to C–H group stretching. Fig. 4 also shows the FT-IR spectrum of decomposition products (TG) above 396 °C and shows only CO<sub>2</sub>.

The identification of remaining gases from TG using mass spectrometry (MS) is extremely sensitive. Some fragmentation patterns in the thermal decomposition process of the compounds studied stand out due to decarboxylation and oxidation of the organic matter, like fragments with mass/charge ratios (m/e) 44 and 45 (MS), consistent with the decarboxylation (COO and/or COOH), respectively. Furthermore, in subsequent steps other fragmentation patterns were observed between 60 and 210 °C (TG), with m/e 44, 45, 52, 68, 76, 92, 105, 118, 122, 123, 131 and 135 attributed to the substances formed in oxidation process of organic matter. Therefore, the fragmentation pattern 76, 92, 105, 118 can be attributed to fragmentation of aromatic ring linked to groups (–CH, –CH=CH–, –CH=CH–CH=, ar–OCH<sub>3</sub>). For temperatures above 480 °C it was observed only fragments with m/e 18, 44 and 45 attributed to elimination of water, CO<sub>2</sub> and CO<sub>2</sub>H, due to oxidative/combustion process. Aiming at illustrating the fragmentation path for better understanding, Fig. 5 is displayed.

### 3.5. Preliminary fluorescence study

Three-dimensional fluorescence spectra for lanthanide compounds, except thulium, are shown in Fig. 6. The compounds were investigated at the temperature of 25 °C under excitation and emission scanning wavelengths in the ranges of 210–600 and 220–800 nm at intervals of 10 nm, respectively. From the results obtained, it was found that the emission intensity in the visible region increases for compounds excited in ultraviolet, so that this

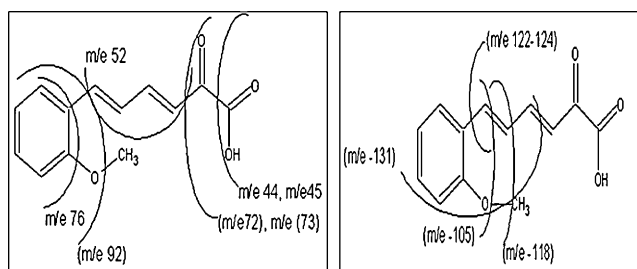


Fig. 5. Fragmentation patterns of the organic ligand from the mass spectrometry data.

behavior is more intense for terbium and holmium compounds. It is also observed that the fluorescence did not result from ultraviolet absorption in wavelengths shorter than 250 nm, since from this point on the radiation is energetic enough to cause the excited states deactivation by chemical bonds rupture.

Regarding the emission wavelength for each compound, from the broad and intense bands it can be suggested that the ligand play an important role in the metal-ligand charge transfer. The ligand–metal energy transfer can probably be derived from a relatively large  $\pi$ -conjugated system of benzene–alkenes of the ligand, which uses the oxygen of the carboxylate and  $\alpha$ -ketonic groups coordinated to the lanthanide ion to benefit the charge transfer [23]. Furthermore, it is possible to assert that the emissions that occur in wavelength different from that one of the sodium salt of the ligand are strong evidences of the bond formed between the ligand 2-methoxycinnamylidenepyruvate and the lanthanide ions. The reason for different spectral shapes probably lies also in the

distinctively different properties of the central lanthanide ion. This contribution is also evident in the FT-IR data presented earlier. Thus, it can be said that the charge transfer occurs from the ligand to the metal center by the antenna effect.

#### 4. Conclusions

From TG–DTA/FT-IR and TG–DTA/MS systems, it was possible to study the compounds and observe that their thermal decomposition and the gaseous products released follow a standard behavior with release of water in the first step, whereas in the following step the carbon dioxide and carbon monoxide release is due to the decarboxylation process of the ligand. The gaseous products like acetone, formaldehyde and methane released in small amounts together with carbon dioxide and carbon monoxide are due to oxidation process of the organic matter, which to the formation of stable intermediate compounds and carbonaceous residues before the formation of the respective metal oxides.

The stoichiometric composition was defined from thermal analysis data, elemental analysis and complexometry like  $M(L)_3 \cdot nH_2O$ , so that hydration water for Tb, Ho and Er compounds was monohydrate or sesquihydrate for Tm, Yb and Lu. For sesquihydrate compounds, the water proportion found is probably due to how the ways in which the water molecules are linked.

From the data of X-ray patterns it is possible to affirm that the compounds were obtained in non-crystalline state as well as from infrared it can be suggested that the metal–ligand coordination is bidentate.

Study of trivalent lanthanide ions coordinated to carboxylate ligands arouses our research group interest once the structure

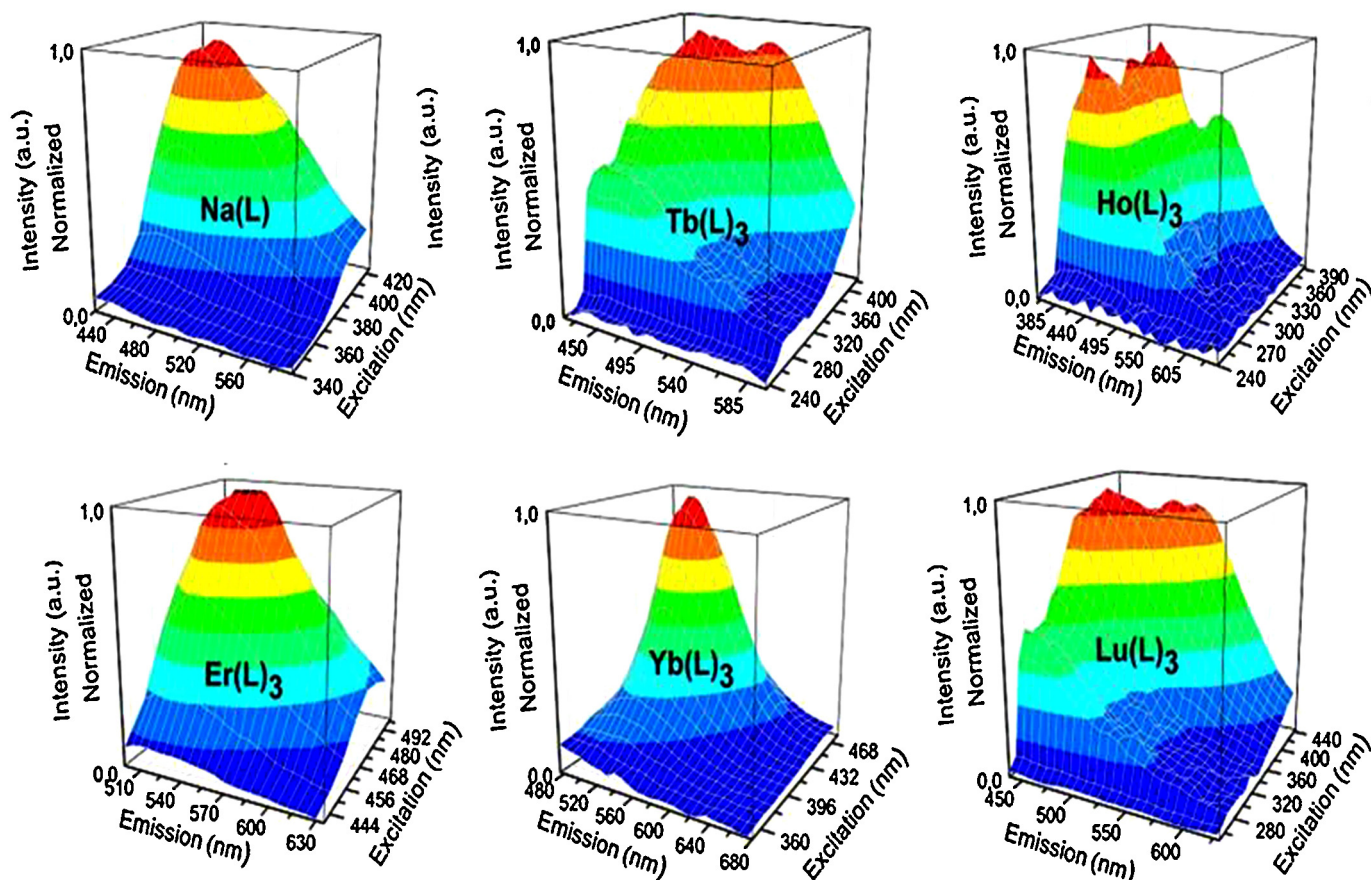


Fig. 6. Three-dimensional fluorescence contour map for lanthanides compounds with 2-methoxycinnamylidenepyruvate ligand and salt under the excitation of 210–600 nm in DMF solution.

of the compound obtained sheds light to its future application or employment in materials modification. Furthermore, preliminary fluorescence studies of compounds obtained with the ligand 2-methoxycinnamylidenepyruvate showed distinct emission and absorption behavior in dimethylformamide. These observations suggest the strong interaction between the ligand and the rare earth ions, as well as the preservation of intrinsic characteristics to rare earth which can enable these compounds characterization by this technique.

### Acknowledgements

The authors thank FAPESP (proc. 97/12646-8), CAPES, CNPQ and FUNDECT Foundations (Brazil) for financial support.

### References

- [1] L. Yichao, Syntheses and photosensitive effects of rare earth carboxylate complexes, *J. Rare Earth*. 14 (1996) 98–104.
- [2] T.A.D. Colman, D.J.C. Gomes, F.J. Caires, O. Treu-Filho, R.C. Silva, M. Ionashiro, Synthesis, thermal and spectroscopic study of light lanthanide nicotinate, in the solid state, *Thermochim. Acta*. (2014), <http://dx.doi.org/10.1016/j.tca.2014.06.013>.
- [3] T.F.A.F. Reji, A.J. Pearl, B.A. Rosy, Synthesis characterization, cytotoxicity, DNA cleavage and antimicrobial activity of homodinuclear lanthanide complexes of phenylthioacetic acid, *J. Rare Earths* 31 (2013) 1009–1016.
- [4] X. Wenmei, W. Qiguang, Y. Lan, Y. Rudong, Synthesis, characterization and crystal structure of tri-aquo bimalonate malonate samarium(III) monohydrate, *Polyhedron* 11 (1992) 2051–2054, [http://dx.doi.org/10.1016/S0277-5387\(00\)83161-7](http://dx.doi.org/10.1016/S0277-5387(00)83161-7).
- [5] E. Hansson, Structural studies on the rare earth carboxylates. 17. The crystal and molecular structure of hexa-aquo tris-malonato di-neodymium(III) dihydrate, *Acta Chem. Scand.* 27 (1973) 2441–2454, <http://dx.doi.org/10.3891/acta.chem.scand.27-2441>.
- [6] O.S. Siqueira, C.B. Melios, M. Ionashiro, M. de Moraes, M. Molina, Complexation of some trivalent lanthanides, scandium(III) and thorium(IV) by benzylidenepyruvates and cinnamylidenepyruvate in aqueous solution, *J. Alloys Compd.* 225 (1995) 267–270 <http://www.sciencedirect.com/science/article/pii/0925838894071373>.
- [7] C.F. Almeida, R.C. Andrade, L.W. Aguiar, F.J. Caires, E.A. Falcão, C.T. Carvalho, Thermal and spectroscopic study of the lanthanide 2-aminoterephthalate compounds in the solid state, *J. Therm. Anal. Calorim.* 117 (2014) 251–258, <http://dx.doi.org/10.1007/s10973-014-3721-7>.
- [8] J.C. Wu, C.W. Jin, D.H. Zhang, N. Ren, J.J. Zhang, A series of lanthanide complexes with 2,3-dichlorobenzoic acid and 2,2':6',2''-terpyridine: crystal structures, spectroscopic and thermal properties, *Thermochim. Acta* 620 (2015) 28–35, <http://dx.doi.org/10.1016/j.tca.2015.09.024>.
- [9] J.F. Wang, F.T. Meng, S.L. Xu, X. Liu, J.J. Zhang, Preparation, luminescence and thermal properties of lanthanide complexes with 2-chloro-4-fluorobenzoic acid, *Thermochim. Acta* 521 (2011) 2–8, <http://dx.doi.org/10.1016/j.tca.2011.03.007>.
- [10] C.T. Carvalho, A.B. Siqueira, E.Y. Ionashiro, M. Pivatto, M. Ionashiro, Synthesis and characterization of solid 2-methoxycinnamylidenepyruvic acid, *Eclét. Quim.* 33 (2008) 61–67.
- [11] C.T. Carvalho, A.B. Siqueira, O. Treu-Filho, E.Y. Ionashiro, M. Ionashiro, Synthesis, characterization and thermal behaviour of solid 2-methoxycinnamylidenepyruvate of light trivalent lanthanides, *J. Braz. Chem. Soc.* 20 (2009) 1313–1319, <http://dx.doi.org/10.1590/S0103-50532009000700016>.
- [12] C.T. Carvalho, F.J. Caires, L.S. Lima, M. Ionashiro, Thermal investigation of solid 2-methoxycinnamylidenepyruvate of some bivalent transition metal ions, *J. Therm. Anal. Calorim.* 107 (2012) 863–868, <http://dx.doi.org/10.1007/s10973-011-1679-2>.
- [13] J.F. Wang, N. Ren, F.T. Meng, J.J. Zhang, Preparation and thermal properties of lanthanide complexes with 2,3-dichlorobenzoic acid and 1,10-phenanthroline, *Thermochim. Acta* 512 (2011) 118–123, <http://dx.doi.org/10.1016/j.tca.2010.09.011>.
- [14] S. Faulkner, S.J.A. Pope, B.P. Burton-Pye, Lanthanide complexes for luminescence imaging applications, *Appl. Spectrosc. Rev.* 40 (2005) 1–31, <http://dx.doi.org/10.1081/ASR-200038308>.
- [15] H.A. Flaschka, *EDTA Titrations: An Introduction to Theory and Practice*, second ed., Pergamon Press, Oxford, 1964.
- [16] M. Ionashiro, C.A.F. Graner, J.Z. Netto, Titulação complexométrica de lantanídeos e ítrio, *Eclét. Quim.* 8 (1983) 29–32.
- [17] M.I.G. Leles, E. Schnitzler, M.A.S. Carvalho Filho, N.S. Fernandes, C.B. Melios, M. Ionashiro, Preparation and thermal decomposition of solid state compounds of 4-dimethylaminocinnamylidenepyruvate with trivalent lanthanides and yttrium, *An. Assoc. Bras. Quim.* 48 (1999) 37–42.
- [18] M.I.G. Leles, C.B. Melios, L.M. D'Assunção, M. Ionashiro, Preparation and thermal behavior of mixture of basic carbonate and 4-dimethylaminocinnamylidenepyruvate with lanthanides(III) and yttrium(III) in the solid state, *Eclét. Quim.* 24 (1999) 29–44.
- [19] E. Schnitzler, W. Costa, C.B. Melios, M.I.G. Leles, M. Ionashiro, Thermal behavior studies of solid state compounds of 4-dimethylaminocinnamylidenepyruvate with alkali earth metals, except beryllium and radium, *Eclét. Quim.* 25 (2000) 31–39, <http://dx.doi.org/10.1590/S0100-46702000000100003>.
- [20] K. Nakamoto, *Infrared and Raman Spectra of Inorganic and Coordination Compounds, Part B, Applications in Coordination, Organometallic, and Bioinorganic Chemistry*, fifth ed., Wiley, New York, 1997, pp. 58–61.
- [21] G.B. Deacon, R.J. Phillips, Relationships between the carbon-oxygen stretching frequencies of carboxylate complexes and the type of carboxylate coordination, *Coordin. Chem. Rev.* 33 (1980) 227–250.
- [22] E. Schnitzler, G. Bannach, O. Treu-Filho, C.T. Carvalho, M. Ionashiro, Solid-state compounds of 2-methoxybenzylidenepyruvate and 2-methoxycinnamylidenepyruvate with thorium(IV), *J. Therm. Anal. Calorim.* 106 (2011) 643–649, <http://dx.doi.org/10.1007/s10973-010-1262-2>.
- [23] D.Y. Ma, L. Qin, Y. Li, Q.T. Ruan, Y.W. Huang, J. Xu, Construction of a new 2D Cadmium(II) coordination polymer based on N- and O-donor ligands: synthesis, luminescence and biological activities, *J. Chem. Crystallogr.* 44 (2014) 63–69, <http://dx.doi.org/10.1007/s10870-013-0484-0>.